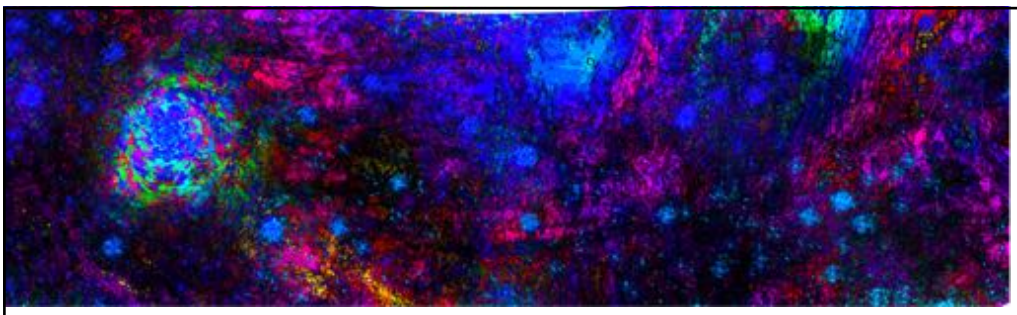

The sky at long wavelengths (as seen with LOFAR)

Ralf-Jürgen Dettmar, Ruhr-University Bochum

with V. Heesen, B. Adebahr, R. Beck, M. Krause,Y. Stein, M. Wezgowiec, A. Miskolczi, George Heald and the LOFAR MKSP & CHANGES teams

1. Motivation

DE605 Jülich

operated by FZJ and RUB

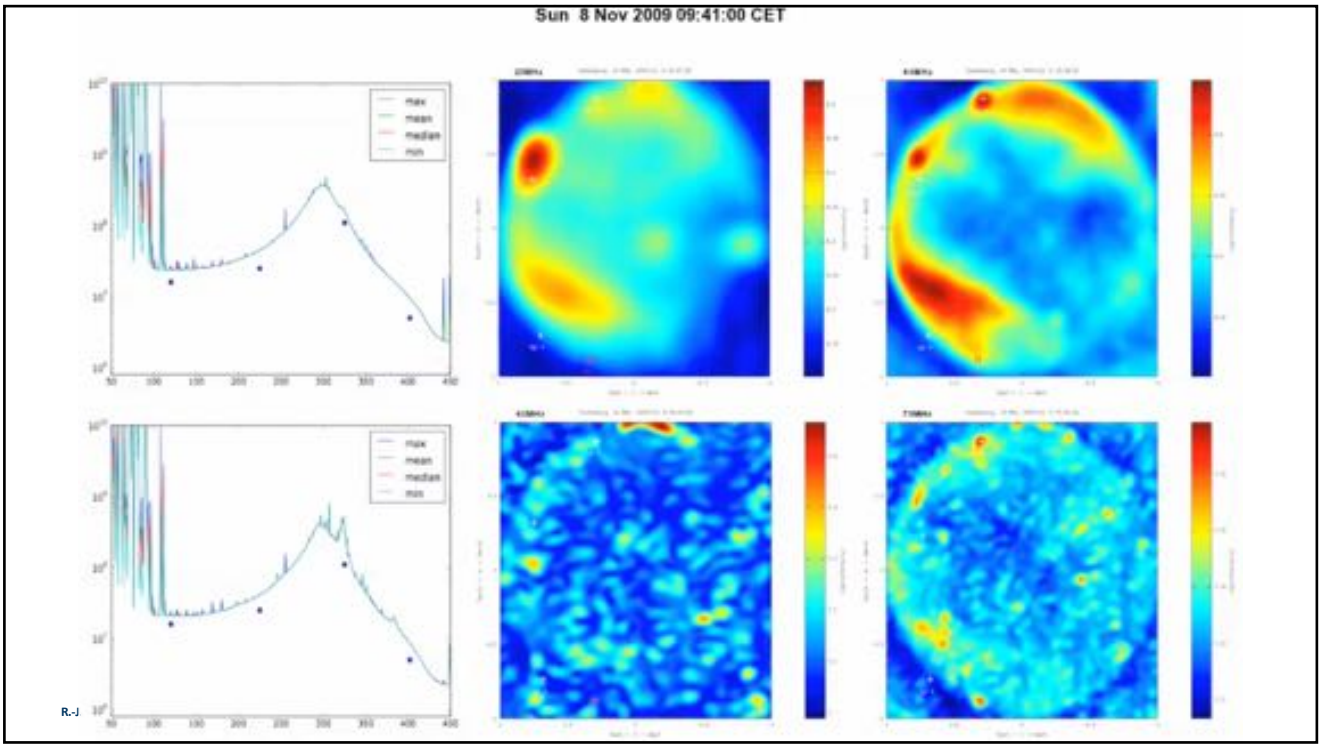

LOFAR (as an example; MWA, LWA)

- Simple antenna design
- No moving parts
- Several simultaneous beams
- Fully digital
- On-line data processing
- Extension over Europe planned

LOw Frequency ARray

20-80 MHz
110-240 MHz

"Silicon" instead of steel, a "digital" telescope

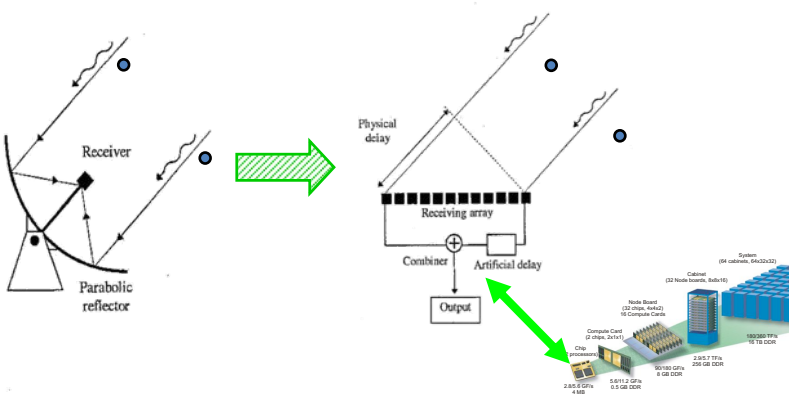

0.5 Tbit/s

25 Tflops

Central field and first international station in Effelsberg

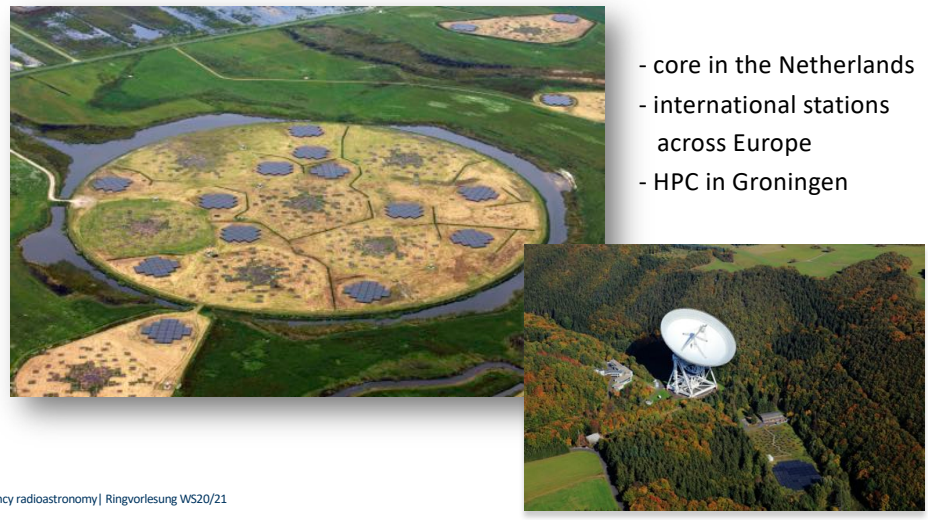

- core in the Netherlands
- international stations across Europe
- HPC in Groningen

LOFAR Antenna

Low Band:
20 – 80 MHz (15m – 4m),
96 antenna per station

High Band:
110 – 240 MHz (3m – 1.2m),
48/96 elements per station,
4 x 4 dipoles per element

LOFAR HBA survey pointing and zoom in for NGC 3556 (discussed later)

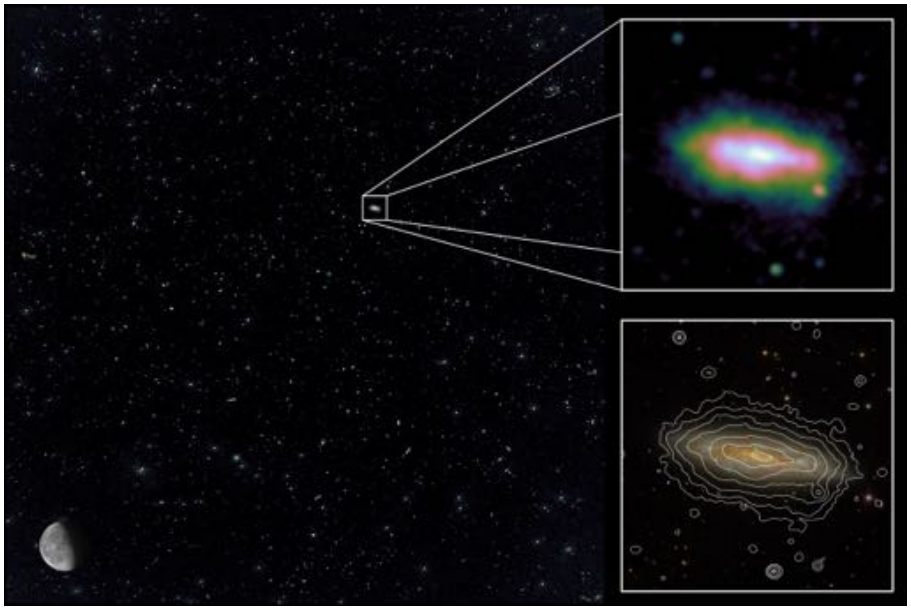

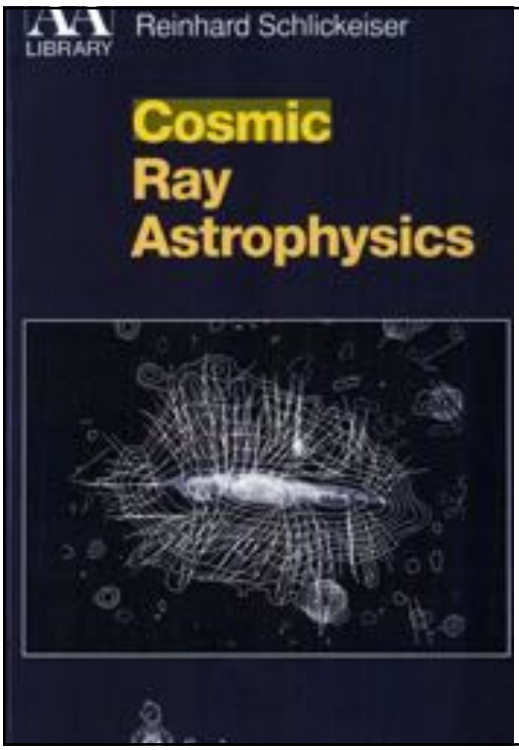

RUB

Connecting cosmic ray astrophysics to radiocontinuum observations of galaxies…

from the lecture by J. Tjus:

Astroparticle Physics

- **Measurements:** photons, cosmic rays & neutrinos
- **Modeling:** Multimessenger approach → explain all signatures at the same time
- **Theory:** Microphysics (hadronic interactions/radiation), Macrophysics (cosmology, plasma physics)

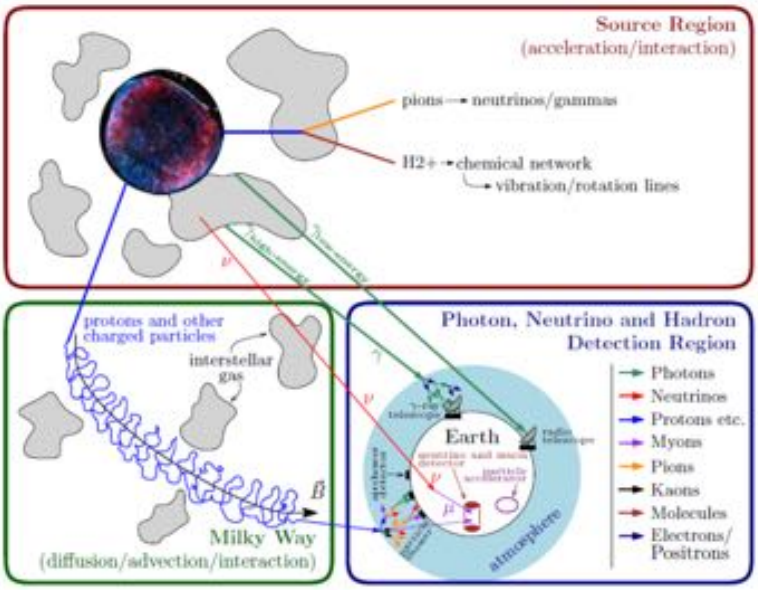

Figure: JBT & Merten, Phys.Rep. (2020)
[legacy of the Wolfgang-Wagner plot, TU Dortmund (2004)]

from the lecture by J. Tjus:

Astroparticle Physics

- **Measurements: photons**, **cosmic rays** & neutrinos,

  Magnetic Fields B !

- **Modeling:** Multimessenger approach → **explain all signatures at the same time**
- **Theory:** Microphysics (hadronic interactions/radiation), Macrophysics (cosmology, **plasma physics**)

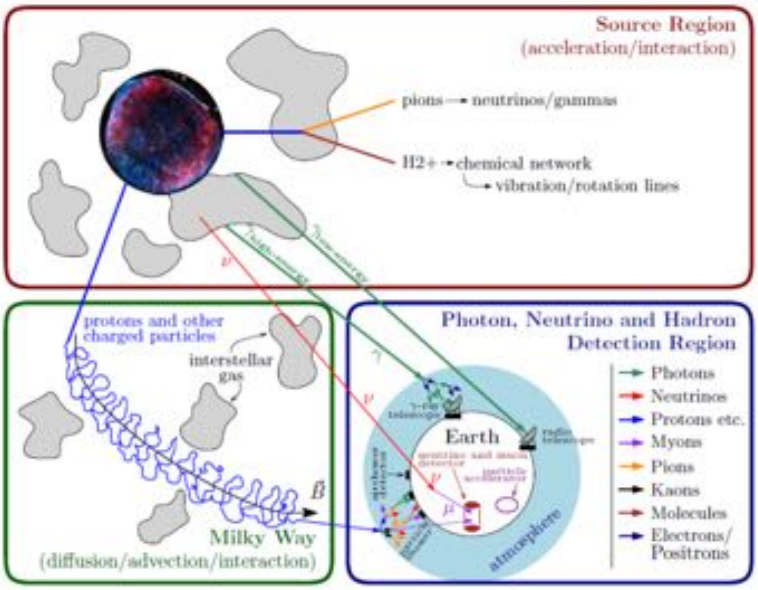

Figure: JBT & Merten, Phys.Rep. (2020)
[legacy of the Wolfgang-Wagner plot, TU Dortmund (2004)]

We have to consider radiation transport !

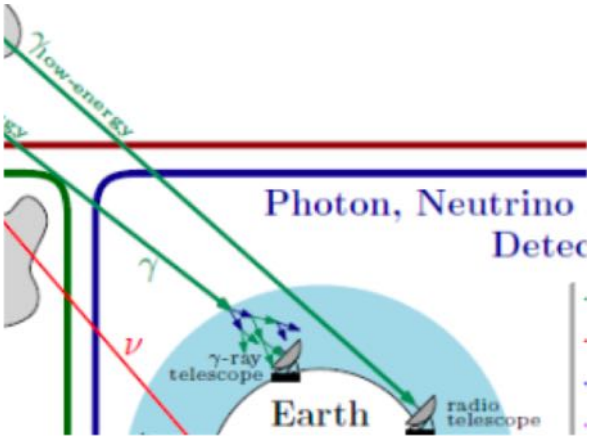

from the lecture by J. Tjus:

RUHR-UNIVERSITÄT BOCHUM

RUB

Frequenzspektrum einer Teilchenpopulation $dN/dE \sim E^{-p}$

- Elektronverteilung $dN/dE = A*E$ [illegible] zwischen E_1 und E_2
- ➔ Von allen Elektronen abgestrahltes Synchrotron-Frequenzspektrum:

$$P_{tot,synch}(\omega) = \int C \cdot F\left(\frac{\omega}{\omega_c}\right) \cdot \frac{dN}{dE} dE \propto F\left(\frac{\omega}{\omega_c}\right) \cdot E^{-p} dE$$

$$\omega_c := \frac{3}{2} \cdot \omega_B \cdot \gamma^3 \cdot \sin\alpha$$

- Gyrationsfrequenz: $\omega_B = \frac{q \cdot B}{\gamma \cdot m \cdot c} \propto \frac{1}{\gamma}$
- ➔ Kritische Frequenz: $\omega_c \propto \gamma^2$

Substitution: $E = \gamma mc^2$ ➔ $x = \omega/\omega_c = \omega/\omega_c(\gamma)$ ➔

1. The non-thermal radio-spectrum and the magnetic field B

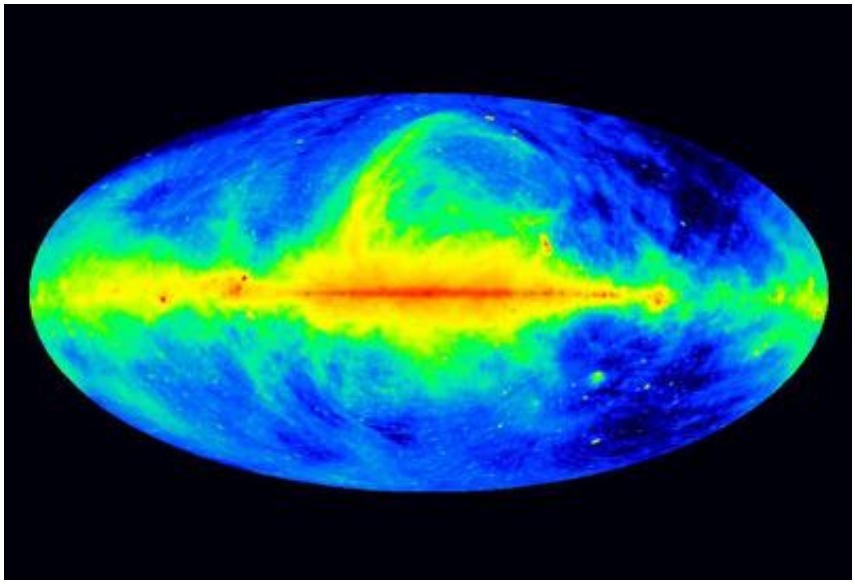

408MHz Jodrell-Parkes-Effelsberg

Synchrotron radiation of relativistic electrons

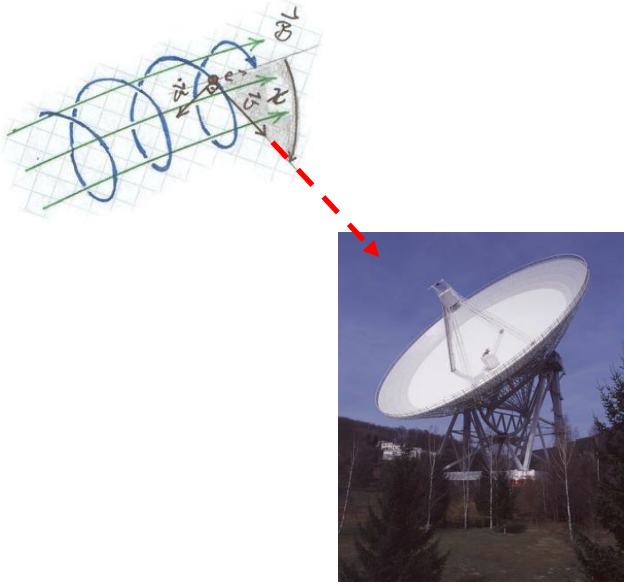

Spectrum of the ensemble:

Convolution of single spectra with energy distribution

$$N(E)\cdot dE \propto E^{-g}\cdot dE$$

$$g = 2\cdot\alpha + 1$$

$$I_\nu \propto B_\perp^{1+\alpha}\cdot\nu^{-\alpha}$$

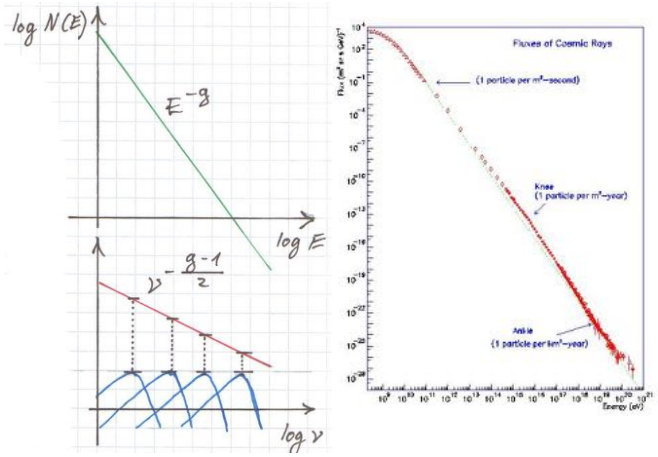

the prototypical starburst M82

Subaru

M82 in X-rays / XMM to scale (Wezgowiec, et al. in prep.)

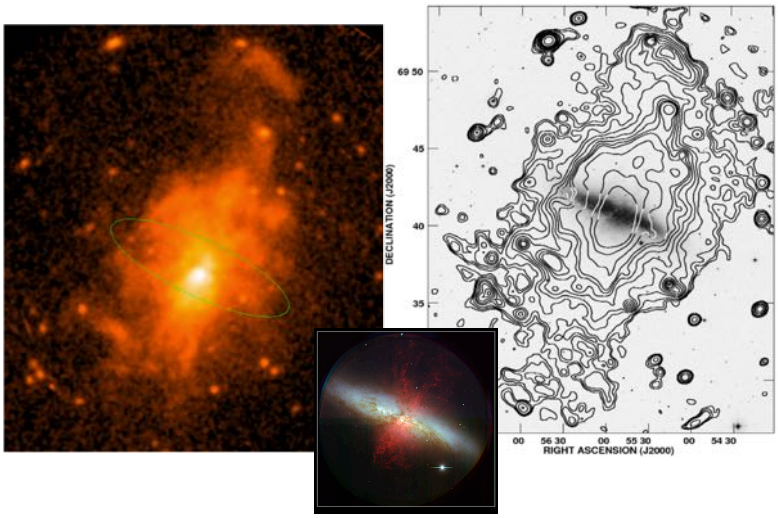

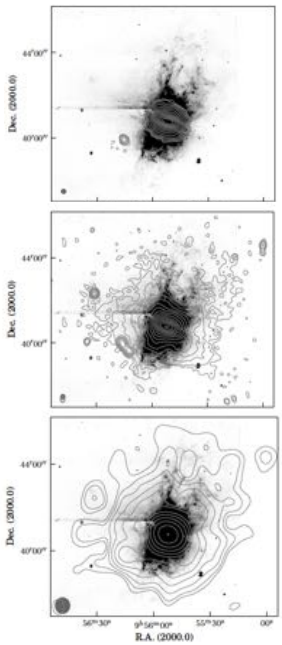

cosmic ray transport in M82

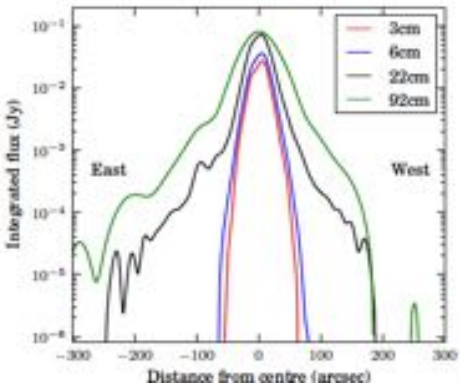

Adebahr et al. 2013, A&A

higher energy electrons radiating at higher frequencies lose their energy faster; lower energy electrons thus travel further, radioemission is more extended

Spectral energy distribution of a spiral galaxy

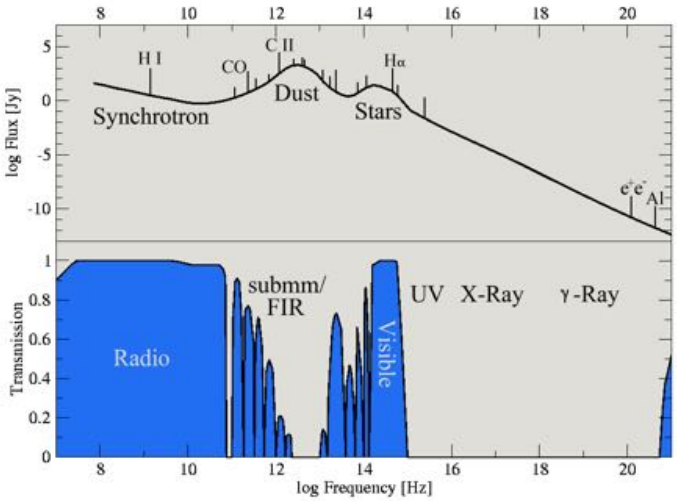

Superposition of continuum radiation processes

Blue: synchrotron
Red: thermal Bremsstrahlung
Green: thermal dust
Violet: spinning dust

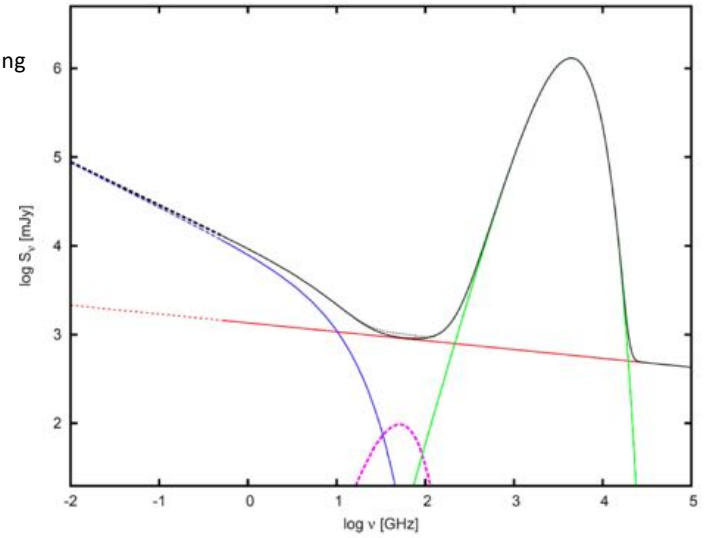

Klein and Fletcher, Springer

Superposition of continuum radiation processes

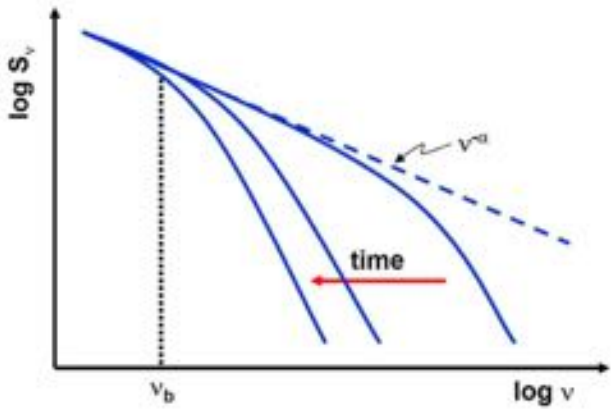

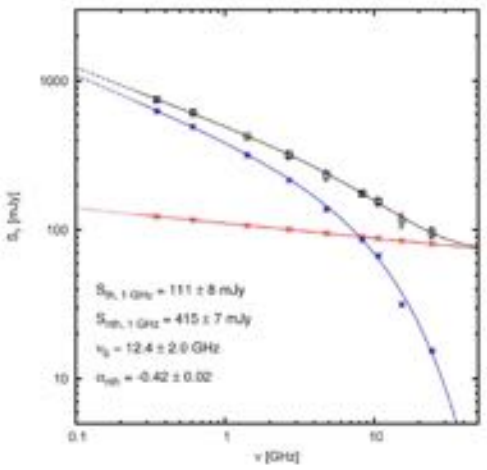

Klein and Fletcher, Springer

auxiliary data:
thermal/non-thermal separation – important for further analysis

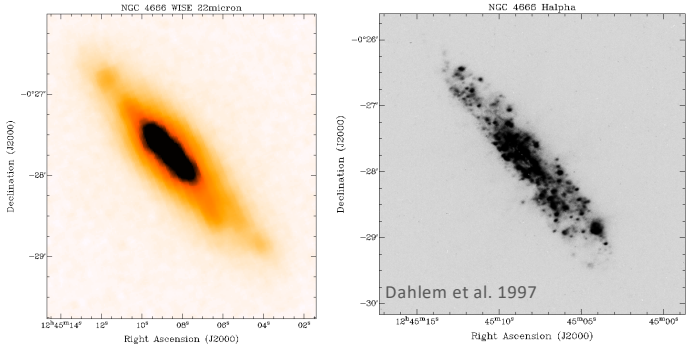

Dust corrected Hα image as thermal emission:

- WISE (22 μm) and Hα (in erg/s)
- Smoothing, regridding
- Calculating thermal Flux based on Calzetti et al. 2007

$F_{thermal} = C\ (L_{H\alpha} + 0.04\ L_{WISE})$

C. Vargas+ 2018. CHANG-ES X: Spatially Resolved Separation of Thermal Contribution from Radio Continuum Emission in Edge-on Galaxies

M82

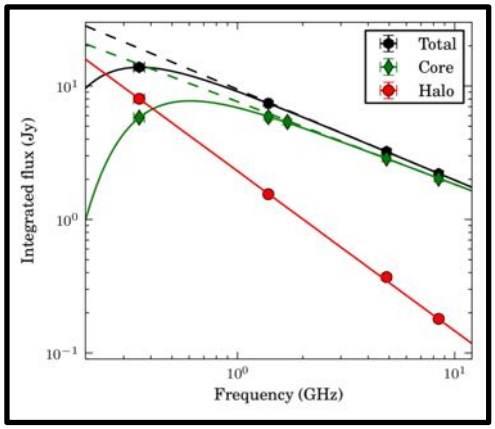

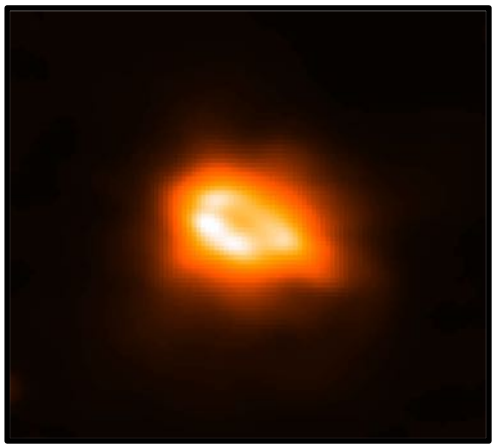

First direct observation of thermal absorption in the diffuse gas of an external galaxy

Energy equipartition => B

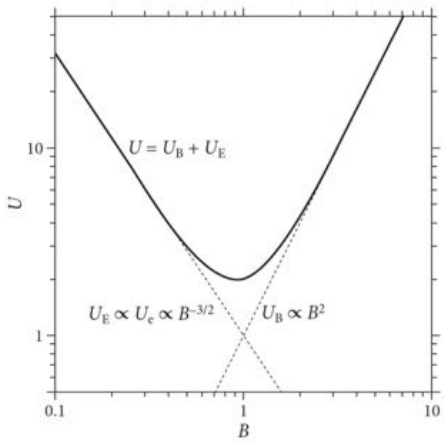

Condon, Ransom, 2016

Figure 5.9. For a source of a given synchrotron luminosity, the particle energy density $U_E \equiv (1+\eta)U_e$ is proportional to $B^{-3/2}$ and the magnetic energy density U_B is proportional to B^2. The total energy density $U = U_E + U_B$ has a fairly sharp minimum near equipartition of the particle and magnetic energy densities ($U_E \approx U_B$).

Processes in the interstellar medium

(from Taylor, Cambridge Univ. Press)

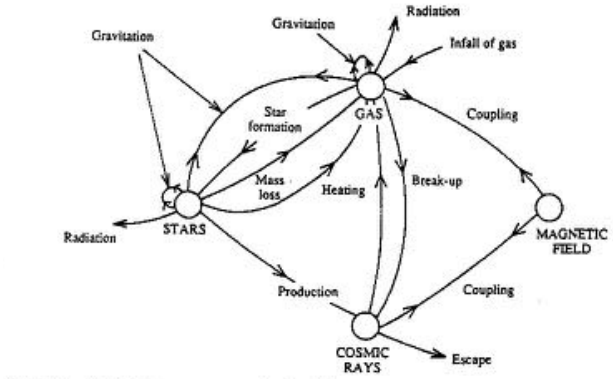

Magnetic Fields and Cosmic Rays contribute significantly to the energy density, or in other terms to the pressure:

$U_{rad} \sim U_B \sim U_{CR} \sim U_{kin}$

2. Cosmic ray electron transport

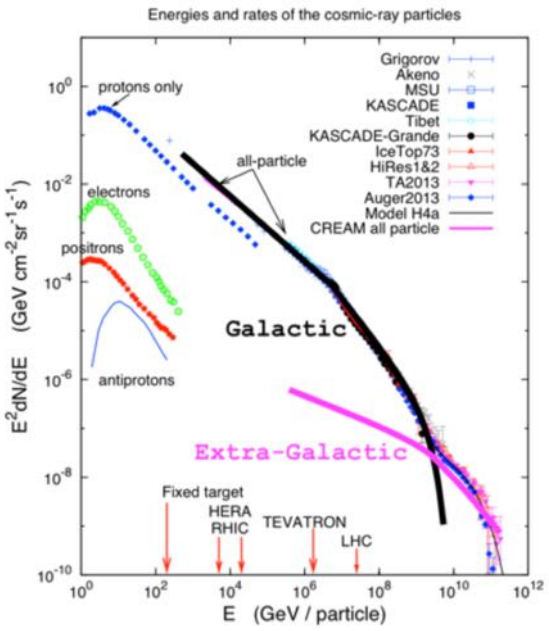

„IceCube Masterclass“

RUHR-UNIVERSITÄT BOCHUM

baryon content of dark matter halos (i.e. galaxies of different mass)

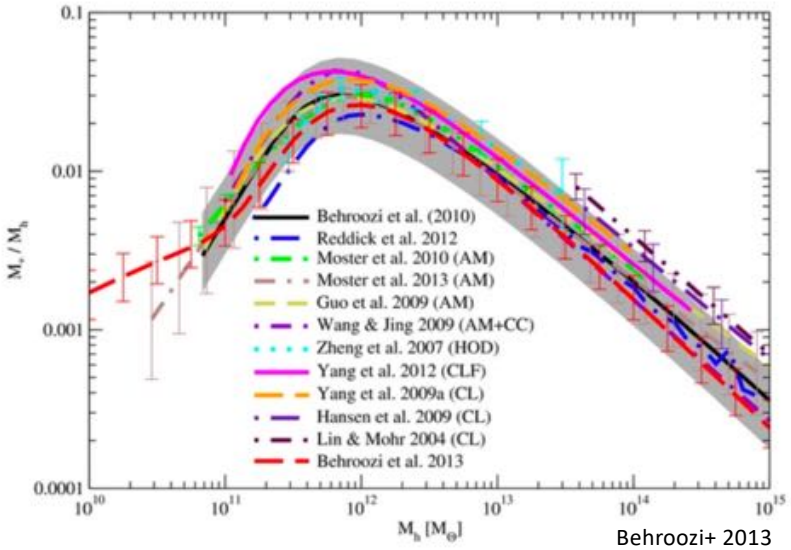

Behroozi+ 2013

RUHR-UNIVERSITÄT BOCHUM

RUB

"feedback" is required in simulations of structure formation

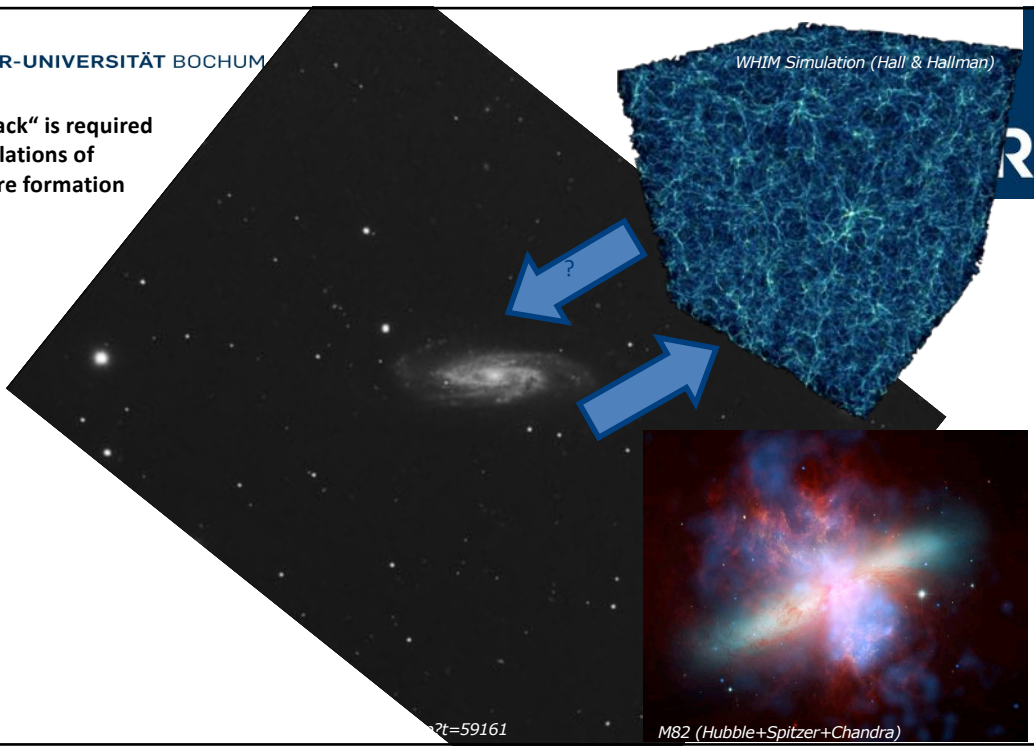

RUHR-UNIVERSITÄT BOCHUM

RUB

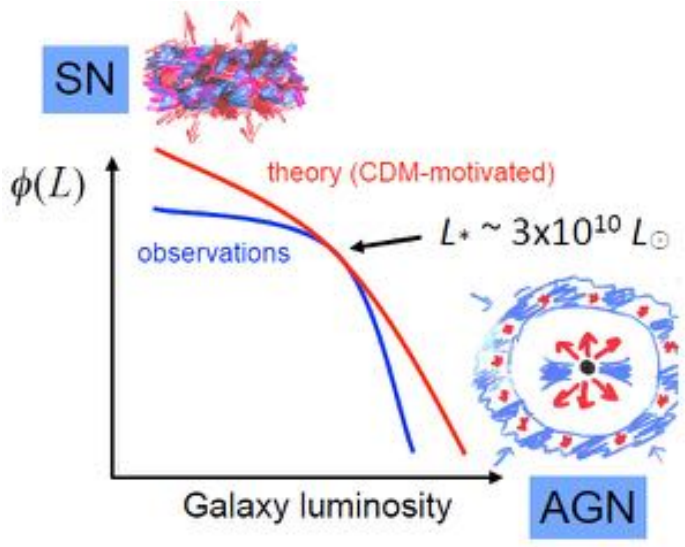

Silk 2013

from the lecture by J. Tjus:

RUHR-UNIVERSITÄT BOCHUM

Leaky-Box Modell

1.) Assumption pure spatial diffusion: $\frac{\partial n}{\partial t} = Q - D\Delta n \approx Q - \frac{n}{\tau_{esc}}$

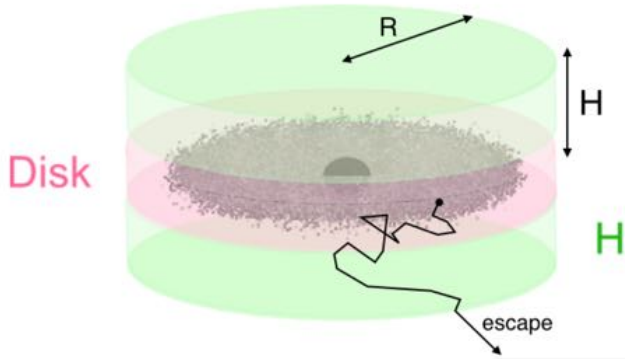

$\tau_{esc} = \frac{D}{H^2}$

2.) Assumption of steady-state: $\frac{\partial n}{\partial t} \approx 0$ ➔ $n(E) = Q(E) * \frac{H^2}{D(E, \delta B/B)}$

What we can measure: synchrotron emission from CR electrons

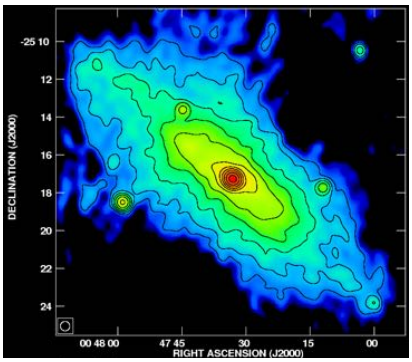

NGC 253 radiocontinuum study at 3, 6, 20, 90 cm

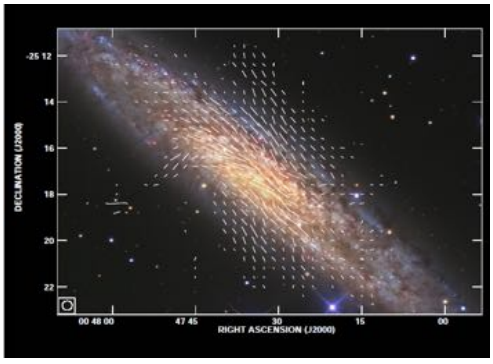

(Heesen, Krause, Beck, Dettmar 2009 A&A)

Polarized emission (and angles):
$I \propto \int n_{CR} B_{\perp}^{1+\alpha} dl$

Faraday rotation measures of the diffuse polarized emission:
$RM \propto \int n_e B_{\parallel} dl$

RUHR-UNIVERSITÄT BOCHUM

RUB

Simulations of the ISM

- **Clustering of Supernovae => Breakout of the gas**

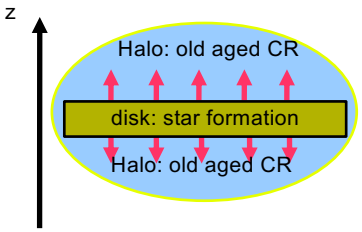

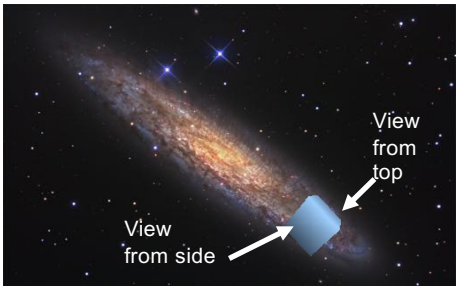

Z is coordinate perpendicular to disk

(V. Heesen)

multiphase ISM in simulations

e.g. de Avillez & Breitschwerdt

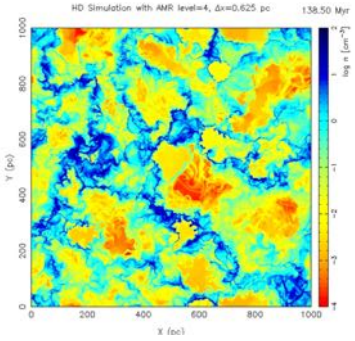

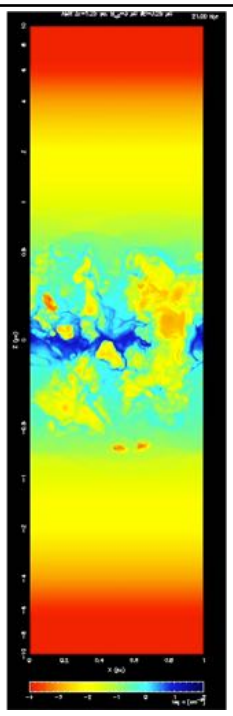

RUB

ApJ 777, L16 (2013)

SIMULATIONS OF DISK GALAXIES WITH COSMIC RAY DRIVEN GALACTIC WINDS

C. M. Booth[1]. Oscar Agertz[2,1]. Andrey V. Kravtsov[1,3,4]. and Nickolay Y. Gnedin[5,1,3]

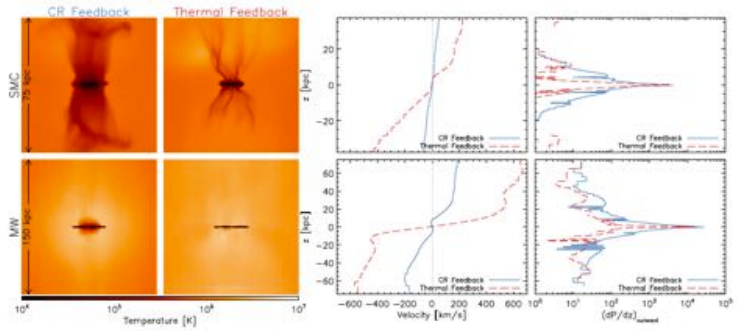

FIG. 3.— Edge-on maps of the temperature in a thin slice around the MW (*top panels*) and SMC galaxies (*bottom panels*) for both the thermal feedback (*left panels*) and CR feedback (*right panels*). CR feedback has a large effect on the temperature structure of the halo gas. The plots show the median velocity (*left panels*) and outward pressure force (*right panels*) as a function of height from the disk for the same two simulations. All quantities are calculated in a cylinder of radius 3kpc, centered on the galactic disk. It is clear that the effect of the CRs is to increase the outward pressure forces in the halo by a factor of 3-5 at all z. This pressure gradient slowly accelerates the wind into the halo. The wind in the thermal feedback simulations is accelerated abruptly from the disk and maintains a constant velocity thereafter.

LAUNCHING COSMIC-RAY-DRIVEN OUTFLOWS FROM THE MAGNETIZED INTERSTELLAR MEDIUM

Philipp Girichidis[1], Thorsten Naab[1], Stefanie Walch[2], Michał Hanasz[3], Mordecai-Mark Mac Low[4,5], Jeremiah P. Ostriker[6], Andrea Gatto[1], Thomas Peters[1], Richard Wünsch[7], Simon C. O. Glover[5], Ralf S. Klessen[5], Paul C. Clark[8], and Christian Baczynski[5] — Hide full author list

Published 2016 January 6 • © 2016. The American Astronomical Society. All rights reserved.
The Astrophysical Journal Letters, Volume 816, Number 2

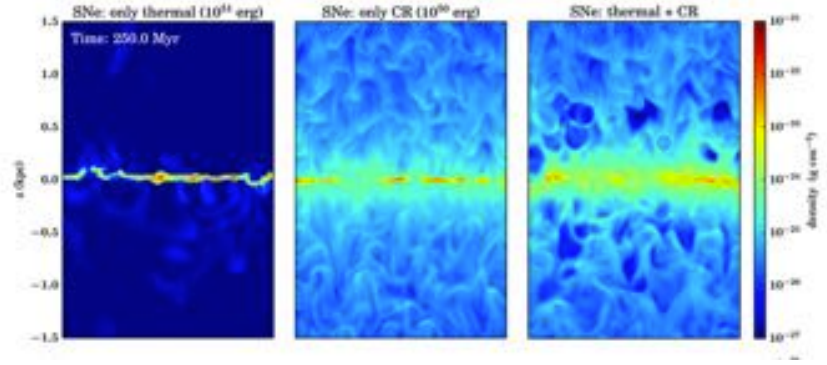

Multifrequency study of NGC 253 (Heesen et al 2009)

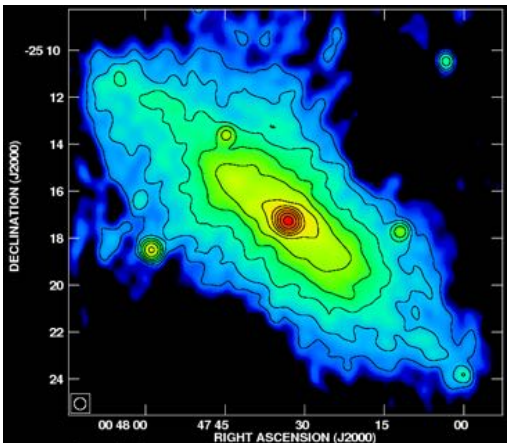

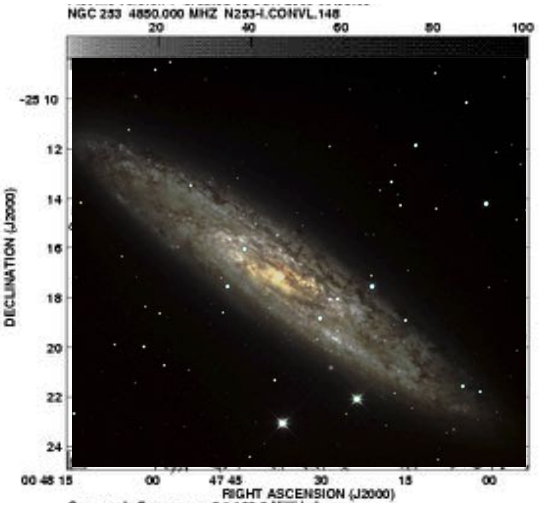

NGC 253 radiocontinuum study at 3, 6, 20, 90 cm

Total magnetic field strength

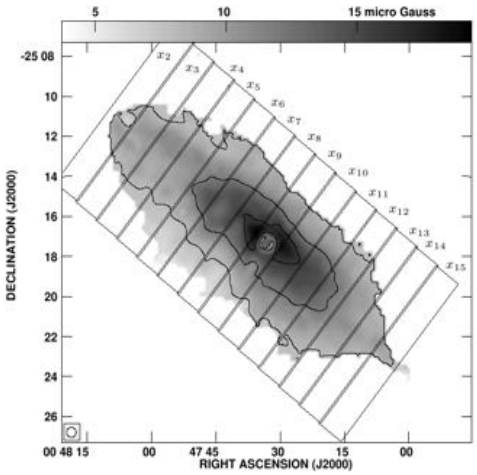

local magnetic field strength

local Synchrotron-lifetime

equipartition magnetic field strength: $B \propto L_\nu^{1/(3+\alpha_{\rm nt})}$

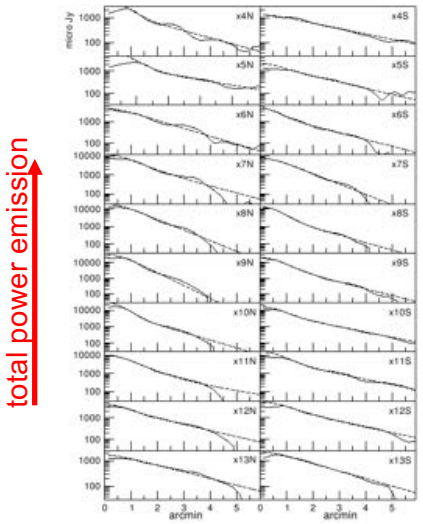

Exponential distribution with scaleheight: h perpendicular to disk: z

typical scaleheight ~ 1.7 kpc

Scaleheight vs. Synchrotron- lifetime

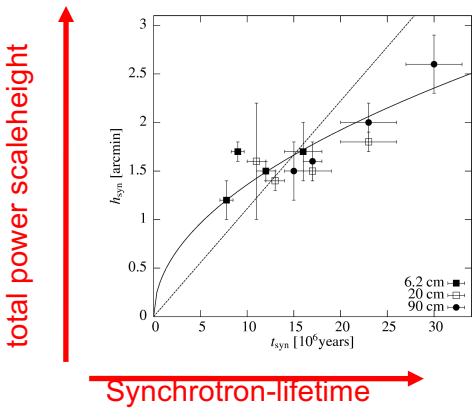

Cosmic ray propagation

$$v_{\rm e} = \frac{3+\alpha_{\rm nt}}{2}\frac{\Delta h_{\rm e}}{\Delta t_{\rm Syn}}$$

$$\bar{v}_{\lambda 6.2} = (280 \pm 40)\ {\rm km\,s^{-1}}$$

close to escape velocity!

analysis of CR transport (ATCA 6&20cm)

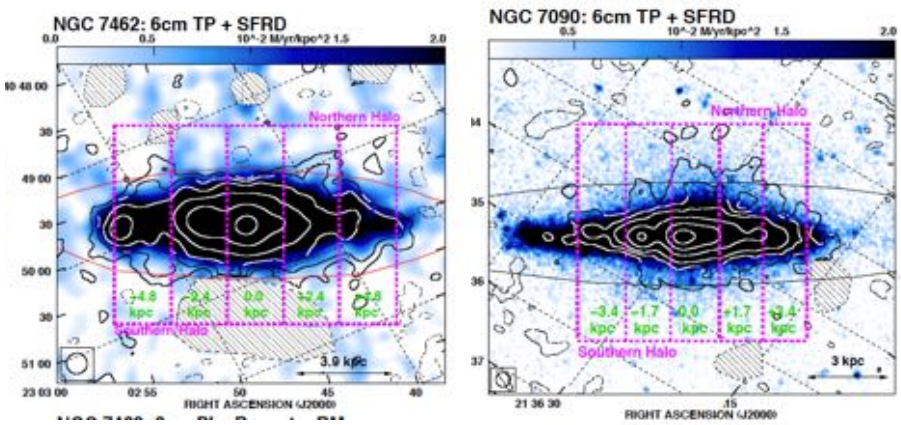

Heesen, Dettmar, Krause et al. 2016 MNRAS 458, 332

"clean non-thermal emission": 1D Modelling of CR–Transport

N(E, z): Cosmic Ray Electron number (column) density

Advection: $$\frac{\partial N(E,z)}{\partial z} = \frac{1}{V}\left\{\frac{\partial}{\partial E}\left[b(E)N(E,z)\right]\right\}$$

Diffusion: $$\frac{\partial^2 N(E,z)}{\partial z^2} = \frac{1}{D}\left\{\frac{\partial}{\partial E}\left[b(E)N(E,z)\right]\right\}$$

CRe losses: $$-\left(\frac{\mathrm{d}E}{\mathrm{d}t}\right) = b(E) = \frac{4}{3}\sigma_{\mathrm{T}} c \left(\frac{E}{m_{\mathrm{e}}c^2}\right)^2 (U_{\mathrm{rad}} + U_{\mathrm{B}})$$

iC losses

synchrotron radiation

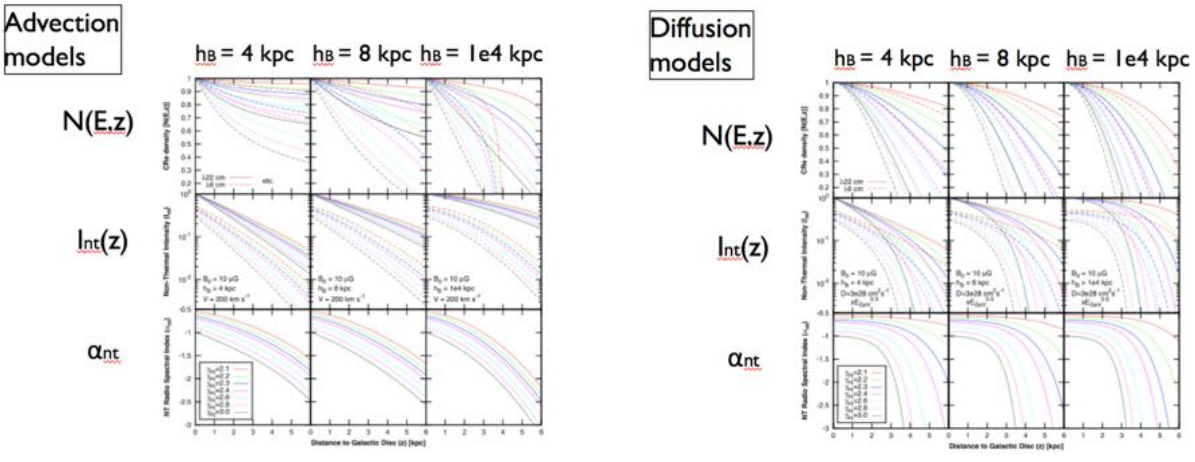

(V. Heesen)

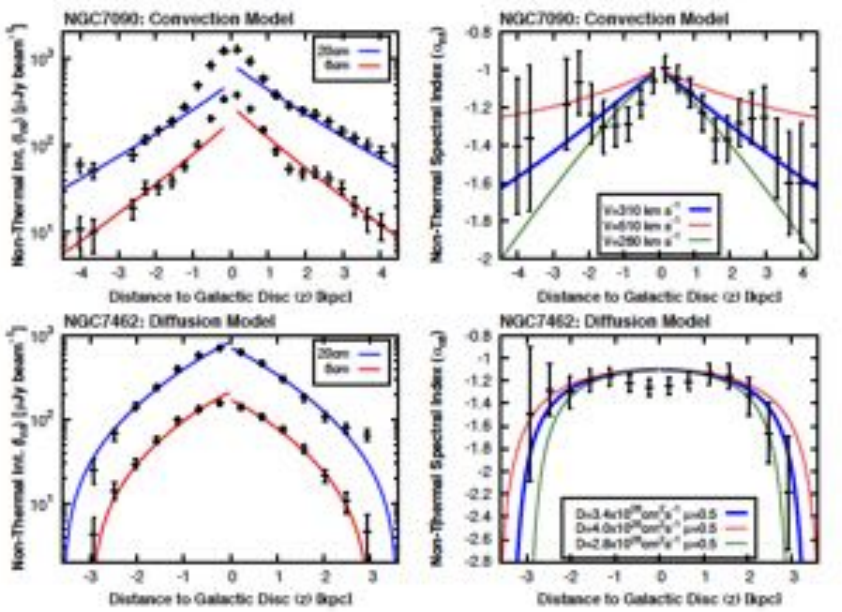

Heesen, Dettmar, Krause et al. 2016 MNRAS 458, 332

Table 2. Observation details for the galaxies presented in this paper.

Galaxy	Band[a]	ν[b] (GHz)	Telescope[c]	Configuration[d]	Project[e]	Time[f] (h)	Date[g]	Notes[h]	Reference[i]
NGC 55	*L*	1.37	ATCA	750D	C287	8.7	1993 Aug 1	Mosaic	17
...	...	...	...	375	C287	11.2	1995 Jan 12	...	...
...	...	...	...	750A	C287	11.1	1995 Oct 25	...	...
...	...	...	...	H75	C1341	5.0	2005 Jul 17	Mosaic	This work
...	...	...	...	EW352	C1341	9.4	2005 Oct 7	...	...
...	*C*	4.80	...	375	C287	3.6	1994 Mar 29	Mosaic	17
...	...	...	...	375	C287	10.2	1994 Mar 30	...	...
...	...	...	...	375	C287	7.8	1994 Mar 31	...	...
...	...	...	...	375	C287	12.5	1994 Nov 23	...	...
...	...	...	...	750A	C287	5.1	1995 Mar 1	...	...
...	...	...	...	375	C287	5.3	1995 Aug 16	...	...
...	...	...	...	375	C287	10.2	1995 Nov 24	...	...
...	...	4.67	...	EW352	C1974	7.6	2008 Nov 22	...	This work
...	...	...	...	EW364	C1974	9.9	2009 Feb 13	...	...
...	*C*	5.60	...	H168	C1974	7.6	2010 Mar 27	...	...
...	*C*	4.80	Parkes	single-dish	P697	16.0	2010 Oct 7	Merged	...
NGC 253	*L*	1.46	VLA	B+C+D	AC278	4.1	1990 Sep–1991 Mar	Mosaic	2
...	*C*	4.86	...	D	AH844	35.8	2004 Jul 4–24	Mosaic	10
...	...	4.85	Effelsberg	single-dish	N/A	N/A	1997	Merged	...
NGC 891	*L*	1.39	WSRT	Multiple	R02B	240	2002 Aug–Dec		13
...	*C*	4.86	VLA	D	AA94	11.2	1988 Aug 29		16
...	...	4.85	Effelsberg	single-dish	44–95	9.1	1996 Feb–Aug		6
NGC 3044	*L*	1.49	VLA	B	AI28	3.1	1986 Aug 1		This work
...	...	...	...	C	AI23	0.8	1985 Jul 25		11
...	...	...	...	D	AI31	1.1	1987 Apr 28/30		...
...	*C*	4.86	...	C	AB676	0.8	1993 Jun 13		4
...	...	...	...	D	AM573	1.1	1997 Nov 6		This work
...	...	...	...	D	AE31	1.0	1987 Apr 28		11
NGC 3079	*L*	1.66	VLA	B	BS44	1.0	1997 Mar 8		This work
...	...	1.41	...	CD	BS44	2.4	1997 Oct 2		...
...	...	1.43	...	C	AB740	1.3	1996 Feb 17		...
...	*C*	4.71	...	C	AC277	3.9	1990 Dec 9		3
...	...	4.86	...	D	AD177	2.5	1986 Jan 16		This work
NGC 3628	*L*	1.49	VLA	CD	AS300	4.3	1988 Mar 25		14
...	...	...	...	D	AS300	8.4	1987 Apr 7		...
...	*C*	4.86	...	D	AK243	7.7	1991 Mar 28		7
NGC 4565	*L*	1.49	VLA	B	AS326	3.8	1988 Jan 29		16
...	...	1.48	...	D	AS326	10.6	1988 Aug 28		...
...	*C*	4.86	...	D	AK424	3.4	1996 Sep 28		6
NGC 4631	*L*	1.37	WSRT	maxi-short	N/A	6.0	2003 Apr 3		1
...	*C*	4.86	VLA	D	AH369	12.1	1989 Nov 22/26	Mosaic	9
...	...	...	...	D	AD896	4.3	1999 Apr 14	Mosaic	12
...	...	4.85	Effelsberg	single-dish	55–94	6.3	1996 Feb–Aug	Merged	6
NGC 4666	*L*	1.43	VLA	CD	AD346	3.5	1994 Nov 20		5
...	...	1.49	...	D	AS199	0.2	1984 Aug 31		This work
...	*C*	4.86	...	D	AD326	12.5	1993 Dec 20/24		5
NGC 5775	*L*	1.49	VLA	B	AI0028	3.2	1986 Aug 1		8
...	...	1.48	...	B	AB492	1.2	1989 Aug 4		...
...	...	1.49	...	C	AH368	3.6	1990 Nov 19/24		...
...	...	...	...	D	AE31	1.9	1987 Apr 27/30		11
...	*X*	8.45	...	D	AD455	13.4	2001 Dec 14		15

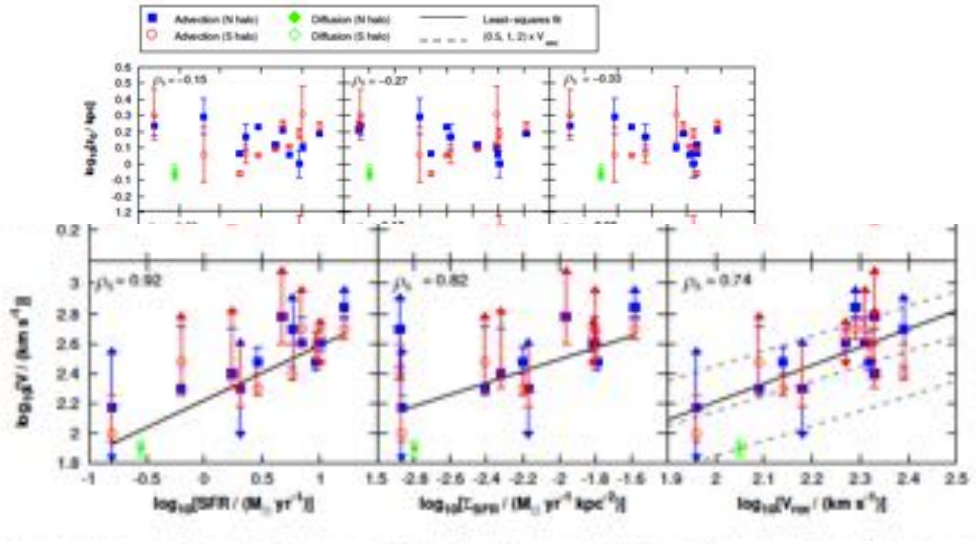

Figure 8. Parameter studies in log-log diagrams as function of SFR, SFR surface density (Σ_{SFR}) and rotation speed V_{rot}. *Top panels*: non-thermal intensity scale height (z_{50}) at 5 GHz (8.5 GHz for NGC 5775) of the thick radio disc. *Middle panels*: magnetic field scale height (h_B) of the thick radio disc. *Bottom panels*: Advection speed (V), where solid lines show least-squares fits. In the bottom right panel the dashed lines show (0.5, 1, 2)$\times V_{rot}$. In each panel, we also present Spearman's rank correlation coefficient, ρ_S, which we derived from values that have both an upper and lower limits.

Heesen+ 2018 MNRAS 476, 158

CRAV (identical to NOCR but 10% of the SN energy in CR energy. The remaining 90% is added as thermal energy. The CR energy can advect with the gas

CRAD is identical to CRAV, but with *anisotropic* instead of isotropic CR diffusion (Pakmor et al. 2016a). The diffusion coefficient in this model is $\kappa = 10^{28}$m^2 s^{-1} parallel to the magnetic field and zero in all transverse directions.

Christine M. Simpson et al. 2016 ApJL 827 L29

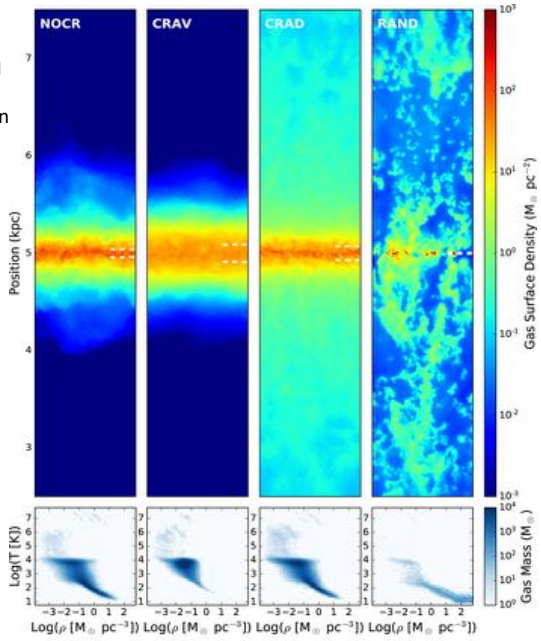

CHANGES:
Continuum HAlos in Nearby Galaxies - an Evla Survey

PI: Judith Irwin, Kingston (ONT/CANADA)

35 edge-on galaxies

inclination > 75 deg
DEC > 25 deg
4 arcmin > D < 15 arcmin
flux > 23 mJy

+ a few well studied larger object

Large proposal 405 hours granted (RSRO)

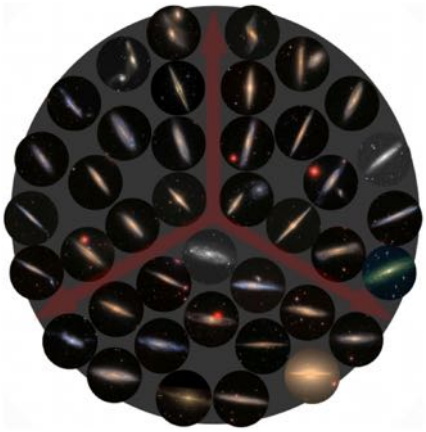

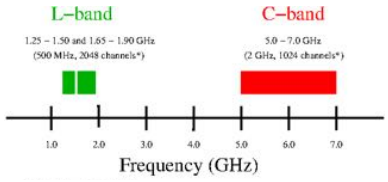

example LOFAR: LoTTS survey

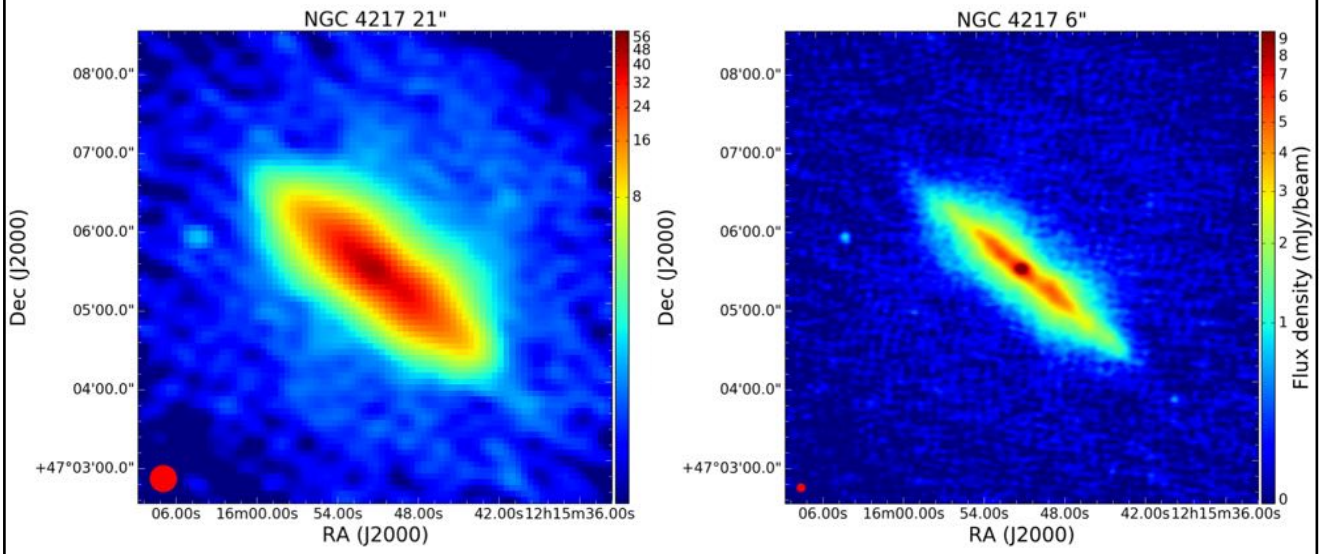

~0.1 mJy rms noise, 0.46Jy total flux (A. Miskolczi)

LOFAR/LoTTS + JVLA

CHANGES XII: N3556 (Miskolczi+ 2019, A&A 622, A9)

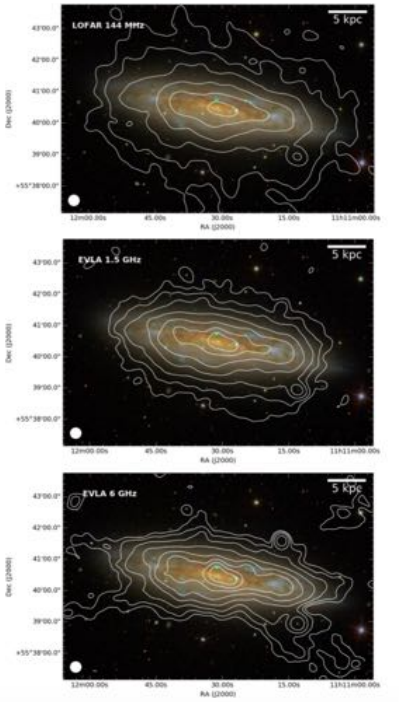

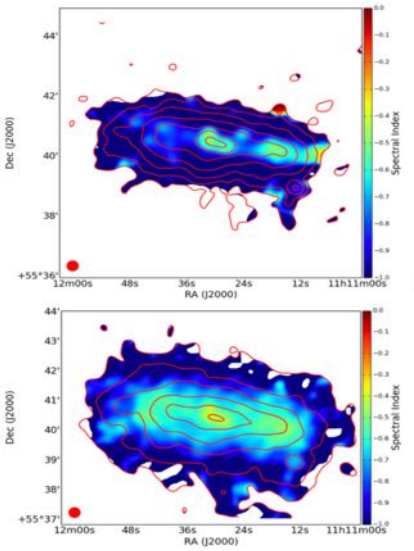

spectral index much better described using a wind profile for v(z)

$$v(z) = v_0 \left(1 + \left(\frac{z}{h_v}\right)^{\beta}\right).$$

LOFAR HBA 10hrs 118-192 MHz (Heald, Heesen, Shridar + LOFAR MKSP)

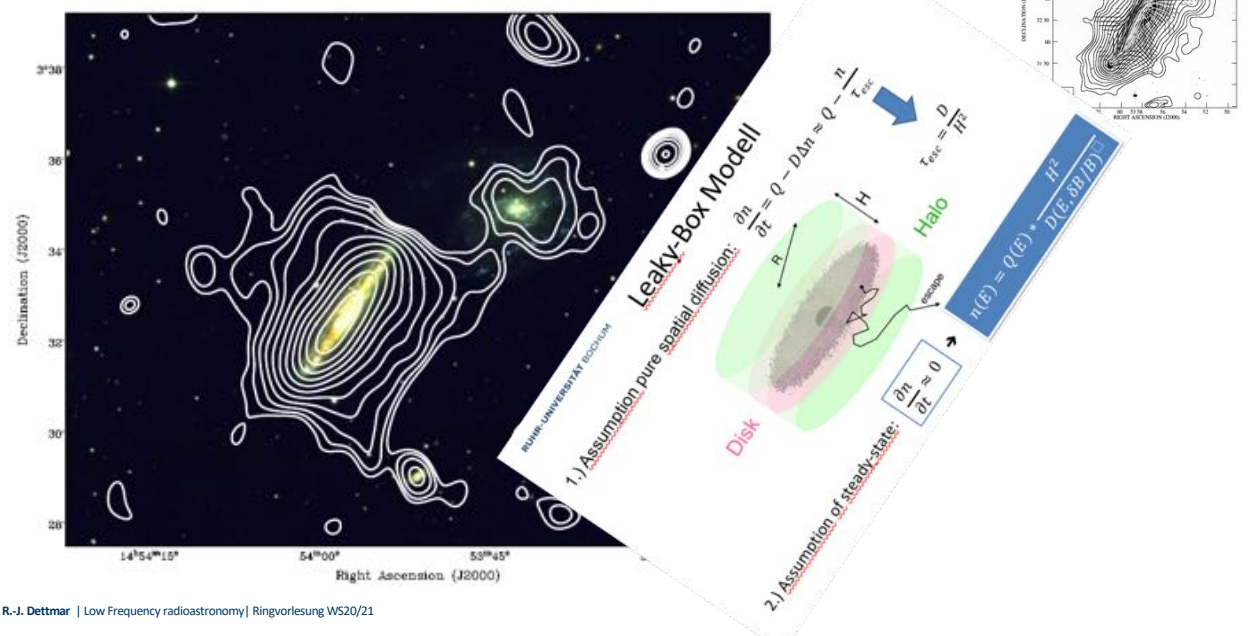

3. Rotation Measure (RM) analysis

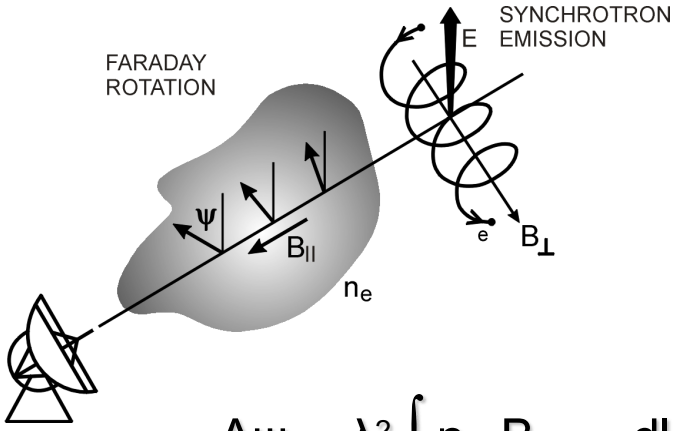

$$\Delta\psi \propto \lambda^2 \int n_e \, B_{reg\parallel} \, dl$$

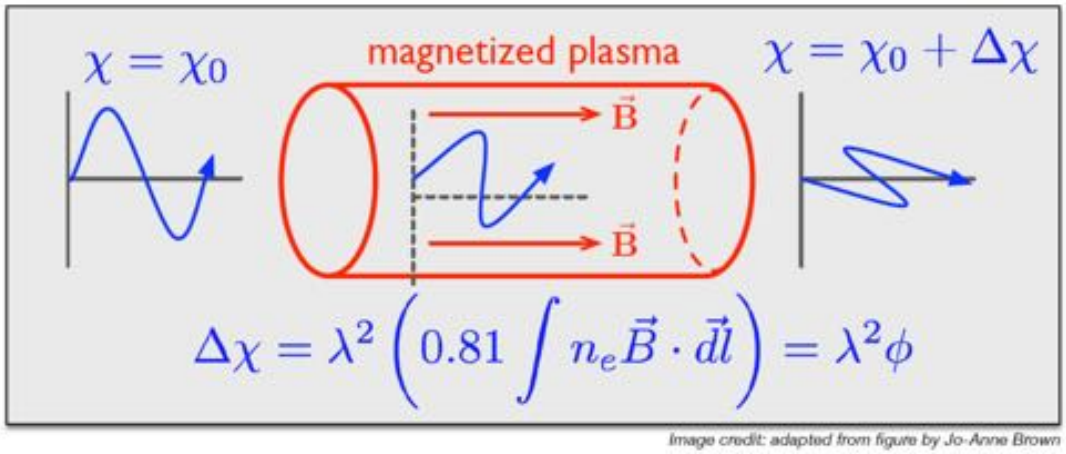

Image credit: adapted from figure by Jo-Anne Brown

with broadband multichannel recievers: rotation measure (RM) synthesis

$$P(\lambda^2) = \int_{-\infty}^{+\infty} pIe^{2i[\chi_0 + \phi\lambda^2]}\mathrm{d}\phi$$

$$P(\lambda^2) = \int_{-\infty}^{+\infty} F(\phi)e^{2i\phi\lambda^2}\,\mathrm{d}\phi,$$

F(f) Faraday dispersion function

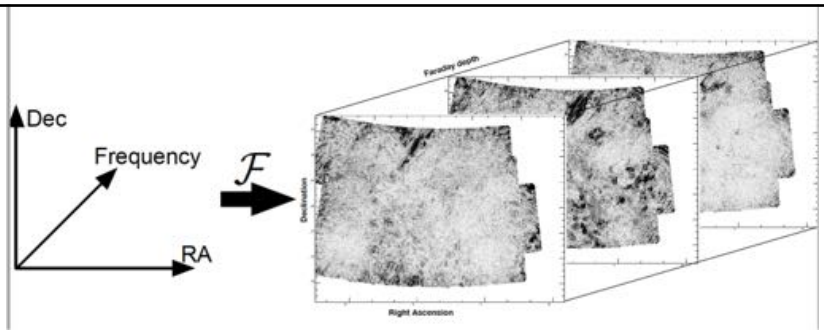

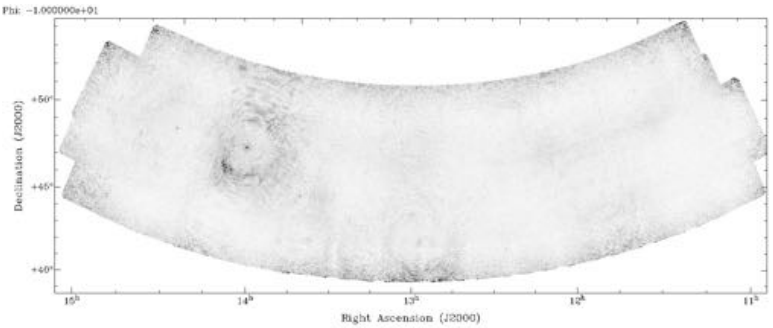

C. van Eck, thesis

WHAT DO WE GET FROM RADIO OBSERVATIONS ?

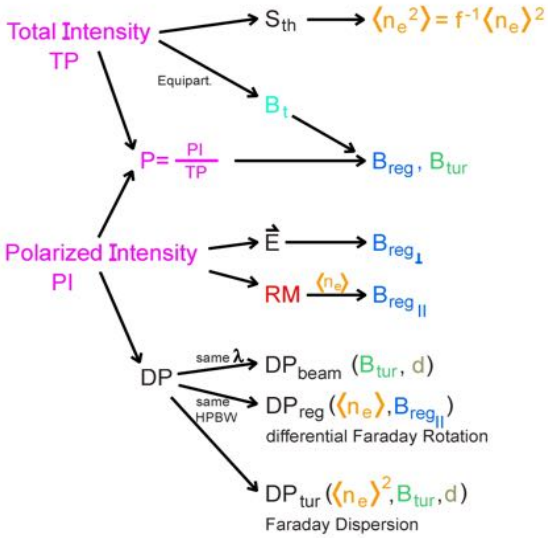

Fig. provided by M. Krause

RUHR-UNIVERSITÄT BOCHUM

RUB

3D-Puzzle Milky Way

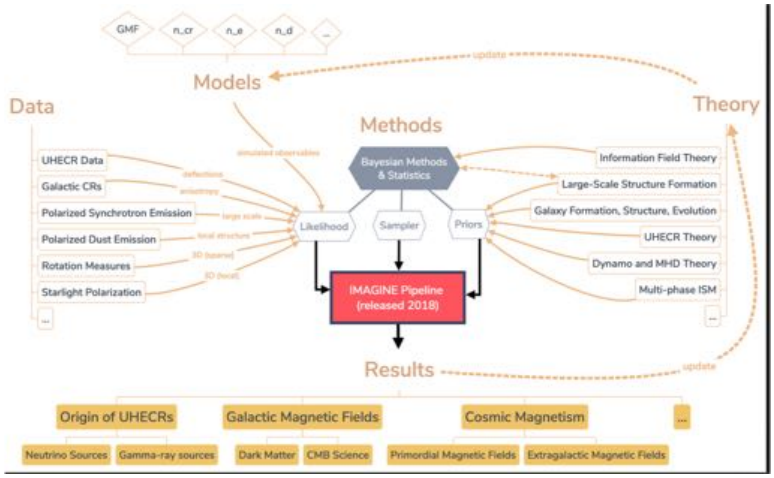

that‘s what is observed for edge-on galaxies:

large scale magnetic field structure in halos

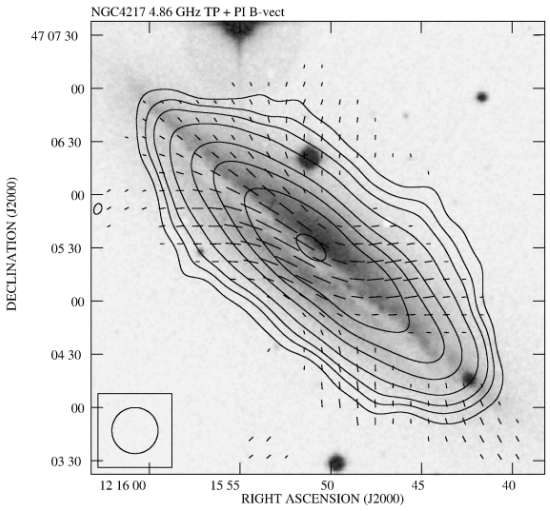

the global magnetic fields in disk galaxies typically have a significant poloidal component !!

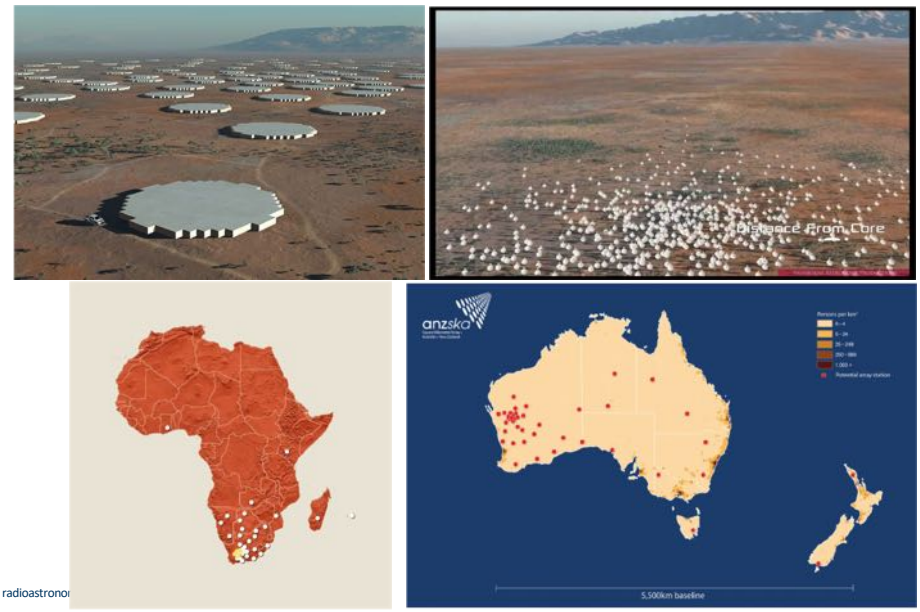

RUHR-UNIVERSITÄT BOCHUM

RUB

Take away messages:

- Observations of the radio-synchrotron provides information on the magnetic field strength and allows to constrain CR propagation models
- CRE transport seems to be dominated by advection in most star forming disk galaxies
- CR driven winds are likely to be important for the evolution of galaxies
- LOFAR observations allow us to study the low energy and „old“ population of CREs
- The Rotation Measure analysis allows us to constrain the magnetic field parallel to the line of sight